applied sciences

MDPI

Article

Topology Optimization of Patient-Specific Custom-Fit Distal Tibia Plate: A Spiral Distal Tibia Bone Fracture

Abdulsalam A. Al-Tamimi

Industrial Engineering Department, College of Engineering, King Saud University, Riyadh 12372, Saudi Arabia; aaaltamimi@ksu.edu.sa

Abstract: Currently, bone fractures are commonly treated with bone fixation plates that present rigid designs and stiff biometals (e.g., Ti-6Al-4V) that increase the probability of stress shielding happening during bone remodeling by shielding the required stress stimuli for adequate healing. This can lead to medical implant loosening, bone resorption and possible bone refracture. In this paper, an initial custom-fit bone plate is designed to be treated based on the computer tomography imaging of a patient suffering from distal tibia spiral fracture. The initial bone plate was redesigned to reduce the risk of bone being stress shielded. Topology optimization were implemented to redesign the bone plates by minimizing the strain energy and reducing the total plate's volume in three different cases (25%, 50% and 75%). A bone-plate construct was assembled and examined using finite element analysis considering load conditions of the patient's gait and the tibia bone being loaded with 10% of the bodyweight. The bone stresses were evaluated in order to compare the topology optimized plates with the initial design. The findings show that with higher volume, load transfer reduction increases in the fractured area and reduces the risk of stress shielding. Topology optimization is a viable approach for building custom-fit distal tibia plates for spiral distal tibia fracture.

Keywords: finite element analysis; long bone fracture; medical imaging; metal bone plates; stress shielding; topology optimization

Citation: Al-Tamimi, A.A. Topology Optimization of Patient-Specific Custom-Fit Distal Tibia Plate: A Spiral Distal Tibia Bone Fracture. *Appl. Sci.* **2022**, *12*, 10569. https://doi.org/10.3390/app122010569

Academic Editors: Maria Paz Morer-Camo, Peris Fajarnes Guillermo and Ramón Miralbés Buil

Received: 23 August 2022
Accepted: 17 October 2022
Published: 19 October 2022

1. Introduction

Currently, metallic fixation medical implants (i.e., plate and screws) are the standard procedure to treat fractured bones for a variety of traumatic and pathological bone disorders [1]. Clinical outcomes showed successful follow-up evaluations [2]. The ideal bone plate scenario is to stabilize the fractured bone fragments with minimal or no interference to the bone remodeling process. However, clinicians and researchers agree that the metallic biomaterials used to build fixation implants for bone treatment have an effect on the bone healing efficiency [3–5]. This is mainly due to the stiffness mismatch between the implant and bone; for example, Ti-6Al-4V elastic modulus is ~120 GPa with a density of 4.43 g/cm^3, whilst cortical bone ranges from 15 to 25 GPa [3]. Wolff's law states that the biomechanical forces subjected to bone will stimulate the remodeling process [4]. Hence, the plate's stiffness strongly influences this process [4,5]. Subsequently, in the bone-plate fracture region, the loads will be distributed unevenly, mainly absorbed by the plate and screws. The bone will be stress shielded from the required stimuli due to the excessive stiffness of the metallic implant, thus leading to decreased mineralization, implant loosening and bone resorption and over the long-term, significant bone density reduction and potential for bone refracture [4,5]. Stress shielding is one of the primary causes of failures in fracture fixation that requires expensive further clinical intervention [6]. Removal of metalwork increases the risk of bone refracture or nerve damage. However, if the fixation is kept in situ, which is not infrequent with adverse reactions such as soft tissue irritation, further stress shielding, growth disturbance and protentional carcinogenic, toxic and allergic reactions can occur [7,8]. This demonstrates how crucial the development of new metallic fixation

implants involving advancements in fixation architecture and materials is to prevent and minimize these issues.

Addressing the elimination or minimization of the stress shielding phenomenon in treating bone fractures is a major research topic. Mainly, these studies are divided into two key research problems focusing on either the fixations materials or the design. Several studies have investigated the incorporation of biomaterials into the implant that have a similar stiffness to bone [9–12]. For example, biodegradable biomaterials have become a major trend in the development of fracture fixations due to their mechanical properties (e.g., Young's modulus of polyglycolic acid is 5–7 GPa) and its ability to degrade while matching the bone healing period and eventually eliminate the risk of stress shielding [9]. However, biodegradable biomaterials show significant limitations when it comes to withstanding physiological loads over a long period and matching the specific biomechanical and degradation performance of bone during healing (i.e., maintaining suitable biomechanics) [10]. Hence, biodegradable biomaterials are more popular in the tissue engineering field due to their more suitable performance in low load-bearing applications (e.g., trabecular bone scaffolds) [11,12].

An ideal design for a medical fixation implant is tailored to optimize its topology, geometry and shape to create a lightweight structure with more flexibility and able to resist physiological loads without any failure. Plate failure is commonly determined by either plastic deformation, crack or plate fracture. It has been demonstrated by several authors that by redesigning the bone plate, stress shielding can be reduced [13,14]. In addition, medical implant design research has shown that patient-specific bone plates provide superior mechanical and biomechanical behavior over the standard computer aided bone plate designs [15]. This assists the preoperative planning preventing, minimizing complications [16]. Furthermore, this route results in improved cost–benefit analysis as the higher quality implants (more accurate anatomical-fit) minimize clinical complications, reduce operating room times, and can eliminate the need for second surgery fixation removal [17,18]. Topology optimization has become a design tool pillar of part shape optimization due to its ability to mathematically generate optimal structures based on the original structure considering a defined objective function (e.g., strain energy) and constraints (e.g., volume and stress). Topology optimization has been shown and proven to be a suitable technique primarily to optimize designs by redistributing the material based on the loading conditions and removing any material regions that have minimum contribution to the design's mechanical stability. The reason why this is optimal for osteosynthesis application is that it can tailor the mechanical stiffness of the plate without changing its parent material and compromise its instability. Since 2006, it has been a popular and feasible approach to design biomedical implants and has been employed in designing joint replacement prosthetics [19], osteosynthesis and reconstruction implants [20,21]. Topology optimization was previously used to address shielding by optimizing the medical implant designs of pelvic prosthetics [22], femur hip joints [23], generic bone plates [24] and spinal cages [25], showing improved bone-implant load transfer. In addition, in the case of [26], the authors presented a topology-optimized mandible fixation plate able to perform and withstand the imposed physiological loads. A topology optimization model of medical implants could be constructed as a stand-alone model without including a bone model to optimize the implant based on its mechanical behavior. However, this will eliminate an important role of the implant's biomechanical behavior. This is why, in this study, topology optimization considered a physiological loading including bone and screws, aiming to minimize the risk of stress shielding. In addition, the adaptation of topology optimization to the patient-specific computer tomography (CT) data is significant in order to optimize plates specific for each patient. This allows medical imaging and topology optimization techniques to integrate, rapidly producing optimized specific plates and accommodating the patient's condition (implant size, injury type, normal or osteoporotic bone, etc.).

However, topology optimization is known to present designs with complex internal/porous structures which are not possible to be manufactured using conventional

techniques [27–29]. Additive manufacturing (AM) is considered to be the ideal technology to fabricate these complex structure; additionally, AM is able to fabricate parts with no complex tooling and achieve a reduction in material waste, and it is significantly reliable in producing medical implants for mass personalization [30–32].

The scope of this study is to combine medical imagining and topology optimization to address stress shielding, promote better load transfer and reduce surgery and post-surgery complications. The purpose of this paper is to present the validity to create a topology-optimized patient-derived custom-fit bone plate. A spiral distal tibia fracture was considered to optimize a distal tibia fixation plate. The custom-fit plate was initially designed considering a computer tomography (CT) scan of a patient's tibia. Afterwards, the plate's initial design was topology optimized considering three volume reductions (25%, 50% and 75%) and a gait loading condition on the CT scanned fractured tibia. Stress finite element analyses were performed to evaluate the initial design and topology-optimized plates to investigate the implant-bone load transfer on the defined bone fracture planes. Finally, a three-dimensionally (3D) printed polymer prototype was fabricated to visualize the optimized plates.

2. Materials and Methods

2.1. Patient Bone Fracture Model and Plate Design

In order to reconstruct the patient's data to 3D digitized model and design a custom-fit distal tibia fixation plate, a ~70 kg female human patient with a spiral distal fractured right tibia (fracture classified 43A1.1) was scanned by computer tomography, as shown in Figure 1 [33]. The patient's bone was dislocated and fractured into two fragments. CT raw data is archived in standard Digital Imaging and Communications in Medicine (DICOM) format. The DICOM format files are then transferred and processed in MIMICS software (Materialise, Leuven, Belgium) for segmentation and obtaining the 3D digital models of the spiral fractured tibia. The 3D digital model was exported as "STL" format and imported and converted as a solid through Autodesk Inventor 2019 (Autodesk, San Francisco, CA, USA) software to be employed in the finite element bone-plate construct model.

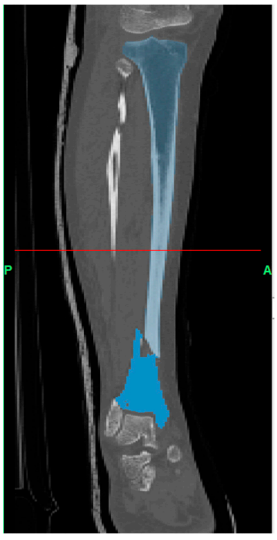

(**a**)

(**b**)

Figure 1. *Cont.*

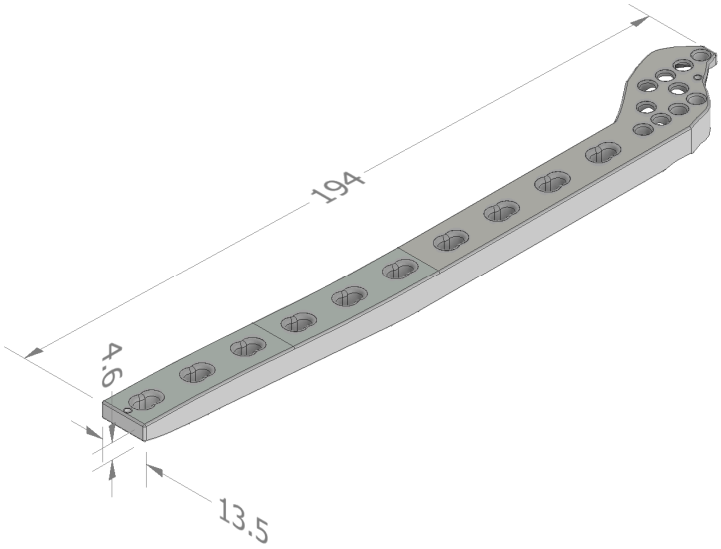

(**c**)

Figure 1. Computer tomography of (**a**) 2D scans and (**b**) 3D bone model and (**c**) initial custom-fit distal tibia fixation plate design, dimensions in mm.

The initial custom-fit fixation plate design 'INT-BP' was created in Autodesk Inventor 2019 (Autodesk, San Francisco, CA, USA) based on the 3D digital tibia bone anatomical data and considered a distal tibia locking compression fixation system to treat a spiral distal tibia fracture with a length of 194 mm, of width 13.5 mm and thickness of 4.6 mm, as shown in Figure 1. Synthes distal tibia locking compression plate (X39.912) was used as a design reference [34].

2.2. Plate Topology Optimization

Topology optimization considers the optimal redistribution of the material of a given design domain to find the optimal element restructure controlled by an objective function and constraints. Solid isotropic microstructure with penalization (SIMP) is a topology optimization approach established by Bendsoe and Sigmund, 1999 [35], employed by several commercial software packages such as Abaqus (Dassault Systèmes, Waltham, MA, USA) and Ansys (Ansys, Canonsburg, PA, USA) and used in medical applications [36]. SIMP aim is to find the optimal design layout considering continuously converging the design variable (material element density, ρ_e) by either retaining the element ($\rho = 1$) or eliminating it ($\rho = 0$) [37].

Mathematical description of the topology optimization problem is as follows [35]:

$$\min_{\rho_e} C(\rho_e) = f^T \cdot u \tag{1}$$

$$\text{subject to } \begin{cases} \sum_{e=1}^{N} (\rho_e) v_e \leq V^*, & (2) \\ \sum_{e=1}^{N} (\rho_e^p) K_e \, u = f, & (3) \\ 0 < \rho_0 \leq \rho_e \leq 1, & (4) \end{cases}$$

where f is the force vector, u is the displacement vector C is the compliance, p is a penalization factor ($p = 3$), v_e is the volume of each element, V* is the volume fraction, K_e is the elemental stiffness matrix and ρ_0 is the initial density. The constraint (3) represents the equilibrium equation representing all the stiffness tensors to attain the material properties of a given isotropic material. The inequality equation in (2) expresses the amount of material at the user disposal with a limited volume for the minimum compliance design. The

constraint (4) presents the interpolation of the density with minimum density to prevent singularities of the equilibrium problem. This design problem for user-defined design domain is formulated as a sizing problem with continuously modifying the stiffness matrix as a function of the material's density. This function becomes the design variable. Due to the material/no material situation, the artificial density intermediate values are penalized in analogous manner. This penalization factor is usually defined as the value of ≥ 3 to obtain globally optimized designs [35]. SIMP method was considered to redesign the implant in Figure 1c, considering 25%, 50% and 75% volume reductions referred to as 'TO25-BP', 'T50-BP' and 'TO75-BP', respectively [37]. Topology optimization problem was executed in TOSCA module, Abaqus (Dassault Systèmes, Waltham, MA, USA).

2.2.1. Finite Element Procedure

In order to achieve custom-fit optimized plate, the finite element analysis in the optimization procedure considered a bone-screw-plate model (i.e., an assembled bone-plate construct) as shown in Figure 2. Although the SIMP approach is not affected by the magnitude of the load, the loading conditions are considered to simulate a 10% bodyweight of the patient's weight (i.e., ~70 N) during swing phase and subjected to the proximal tibia region (Figure 2a) [37–39]. The distal tibia region was fully constrained in order to prevent the model floating. Following the standard practice of fracture fixation, two different screw configurations (i.e., location and number of screws) was considered (Figure 2c,d) [40]. The screw configuration is expected to influence fracture stability and topology optimization procedure [40]. The locking head screws were modelled in Autodesk Inventor 2019 (Autodesk, San Francisco, CA, USA), each screw has a 3.5 mm diameter head and a main body of 2.5 mm in diameter and 35 mm in total length. For simplicity, screw threads were neglected. Fixation plate and screws were applied with an elastic modulus of 120 GPa, and a Poisson's ratio of 0.3, assuming Ti-6Al-4V as the material. In terms of the bone, only the cortical region was considered in this simulation with a Young's modulus of 18 GPa and a Poisson's ratio of 0.3 [41]. The implant holes, screws and bone models were considered as non-design regions. Based on a previous mesh convergence study [24], all models in the finite element analysis considered quadratic tetrahedron elements C3D10, and the considered number of elements is shown in Table 1. In order to simulate the no friction or contact of the Locking Compression Plate technique, a gap of 0.5 mm was imposed between the bone and plate. The screw head were securely locked (i.e., tie-contact) to the plate, and the bone was secured to the screws [41].

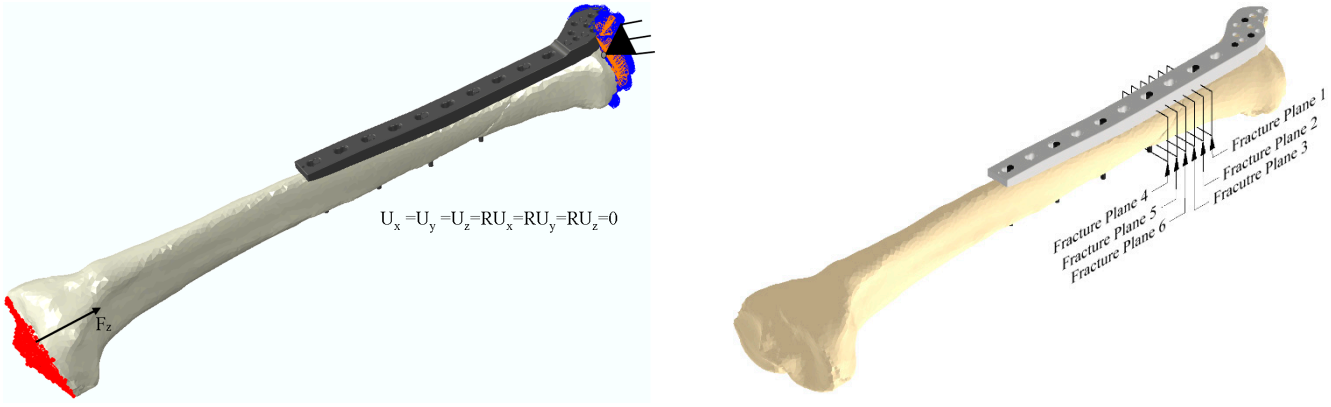

(**a**) (**b**)

Figure 2. *Cont.*

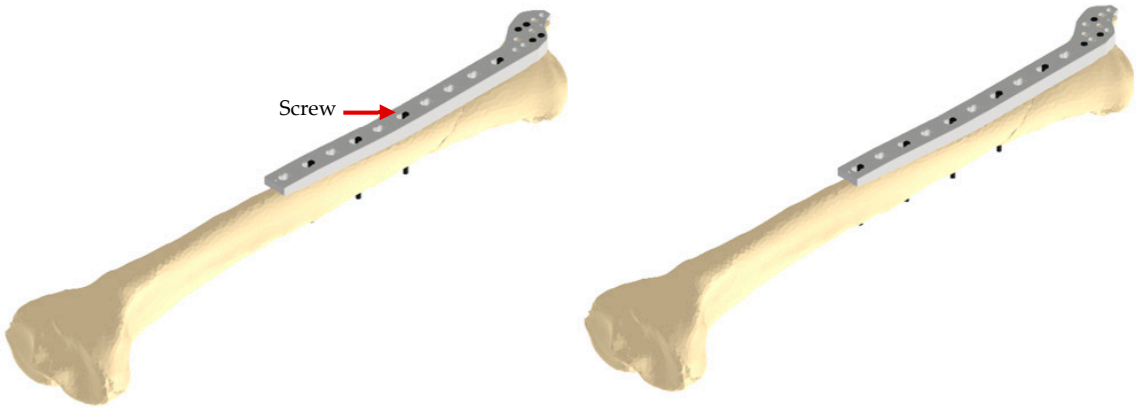

(**c**) (**d**)

Figure 2. Bone plate construct model showing (**a**) loading and boundary conditions, (**b**) fracture planes (distance between each plane is 6 mm) considered to calculate the average bone stresses, (**c**) screw configuration 1 (SC1) and (**d**) screw configuration 2 (SC2).

Table 1. Number of elements considered for each model.

Model	Number of Elements
Bone plate	400,000
Screws	500
Tibia bone–Proximal	87,000
Tibia bone–Distal	29,000

2.3. Bone Plate Stiffness Analysis

The mechanical stiffness was investigated in order to compare both the initial and topology-optimized bone plate designs through finite element analysis considering quasi-static elastic behavior. The bone plate models were assumed homogeneous and isotropic. Similarly to Section 2.2.1, material and mesh properties are considered. The bone plate equivalent stiffness was determined according to the British Standards of bone plates (BS 3531-23.1:1991 ISO 9585:1990) considering a four-point bending setting [42]. As shown in Figure 3, the roller diameter is 10 mm, the span length between the support and force nodes (h) is 15 mm, and the distance between the force nodes (k) is 31 mm. The equivalent stiffness is calculated as follows:

$$E = \frac{\left(4h^2 + 12hk + k^2\right) S.h}{24} \left(\mathrm{N.m^2}\right) \tag{5}$$

where S is the stiffness and is defined through the following equation:

$$S = \frac{RF}{D} \cdot (\mathrm{N/m}) \tag{6}$$

where RF is the average reaction forces along the plate's thickness, and D is the displacement in the maximum tension region.

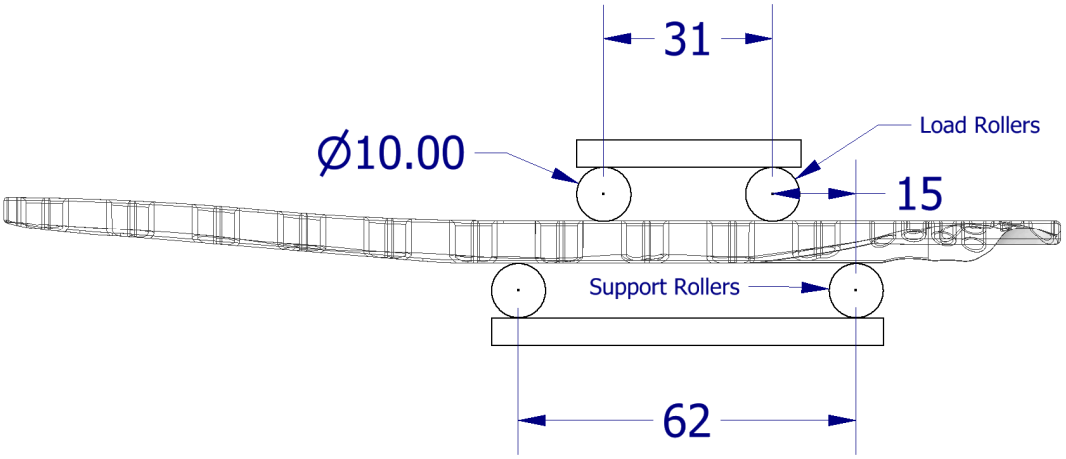

Figure 3. Four-point bending condition of 'INT-BP' plate, dimensions in mm.

The change in percentage in the equivalent bending stiffness between the initial bone plates and topology-optimized bone plates is determined as follows:

$$\Delta\text{equivalent bending stiffness } (\%) = \frac{\left(Stifness^{INT-BP} - Stiffness^{TO-BP}\right)}{Stiffness^{TO-BP}} \quad (7)$$

2.4. Stress Analysis of a Bone-Implant Model

In order to measure load transfer on the bone, the initial design of the distal tibia plate and its topology-optimized counterparts were analyzed and compared numerically considering similar loading and boundary conditions considered in the optimization procedure. The stress on the bone was determined considering six cross sections (i.e., fracture planes) in the fracture area, as shown in Figure 2, and an average stress was calculated. The stress change is defined as follows:

$$\Delta Stress(\%) = \frac{\left(Stress^{INT-BP} - Stress^{TO-BP}\right)}{Stress^{TO-BP}} \times 100 \quad (8)$$

Plate stability post-operation is important and is affected by the tensile strength of the material. The bone fixation plate stability is investigated and their mechanical strength was analyzed using the resulting Von Mises stresses considering the material's yield strength (Ti-6Al-4V ~860 MPa) [5].

2.5. The 3D Printing of the Plate Prototype

A prototype of the plates was visualized for presurgical planning purposes using a fused filament fabrication (FFF) 3D Printer (Raise3D E2, Irvine, CA, USA). After obtaining the designs from topology optimization, the files afterwards were tessellated as an STL format and imported into ideaMaker 4.1.1 (Irvine, CA, USA) to pre-process the design file and define the process parameters. The material used to fabricate the plate prototype was polylactic acid (Raised3D Premium PLA filament; obtained from Raise3D, Irvine, CA, USA). The nozzle diameter used was 0.4 mm, with infill 10%, layer thickness of 0.1 mm, a printing speed of 50 mm/s, melting temperature of 200 °C and bed temperature of 45 °C. All plates were printed in a horizontal orientation.

3. Results and Discussion

In this study, the results show that it is possible by using topology optimization and medical imaging to create less stiff plates with the ability to improve bone healing through anatomical-fit design and by promoting better load transfer to the bone fracture area. Furthermore, the optimized plates have shown to withstand physiological loads.

3.1. Topology Optimization of Bone Plate

Topology optimization model was considered to tailor the strength-to-weight ratio by maximizing the stiffness while reducing 25, 50, and 75% of the initial volume of a custom-fit distal tibia bone plate 'INT-BP'. The aim is to reduce as much volume as possible without risking plate instability to minimize the overall equivalent stiffness. Topology optimization for each screw configuration resulted in three different optimal designs, as shown in Figure 4. Consistent with other findings, the resulting designs align with the stresses distributed from the considered loading and boundary conditions, hence presenting non-uniform designs [20,37]. The results reported an acceptable volume from all obtained designs within less than 5% of the user-defined volumes. Designs considering higher volume reductions have been shown to remove the entire connection between some of the screw holes (e.g., TO75-BP), thus decreasing the number of screws in the plate.

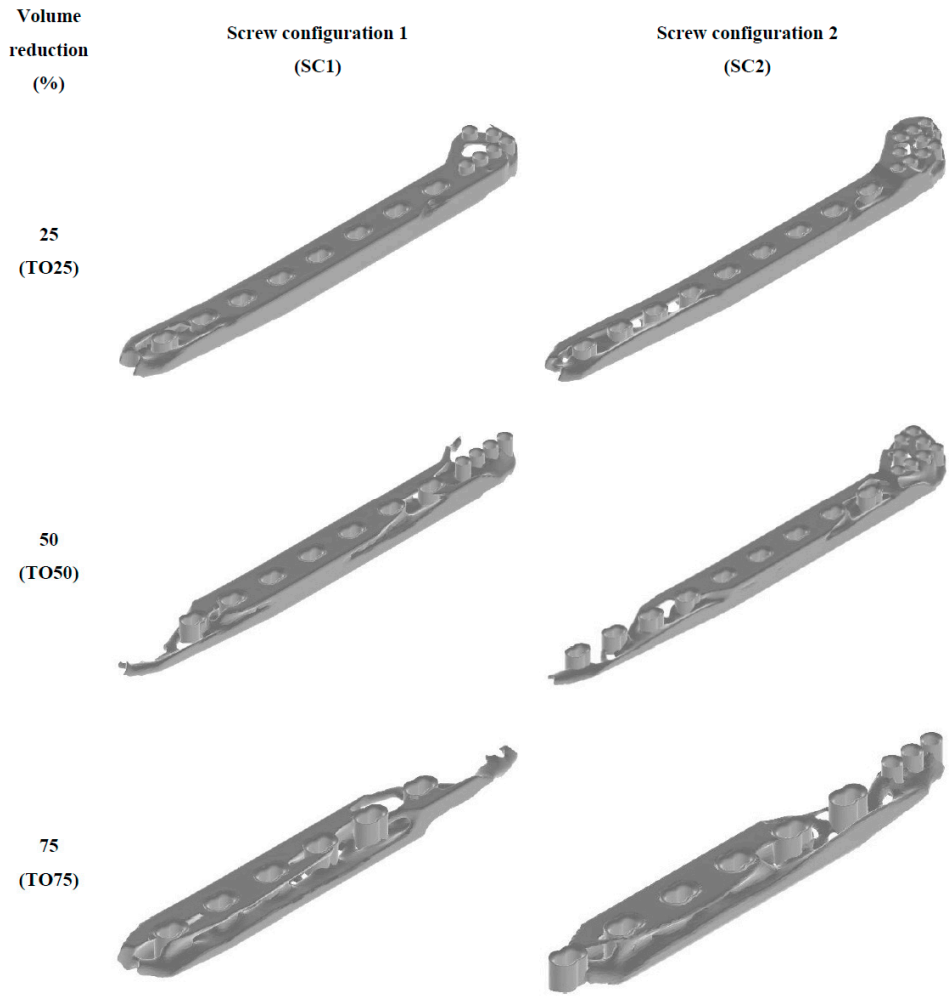

Figure 4. Topology optimization of a custom-fit distal tibia plate under two different screw configurations.

3.2. Plate Mechanical Stiffness

Biomechanically, the tibia bone and plate will be subjected to compression and bending loads during fixation of a tibia shaft, while the plate is fixed on the tension side of the fracture [43]. Furthermore, four-point bending targets the bone plate to withstand compression on one side and tension on the other, longitudinally. Thus, the plates were investigated mechanically considering a four-point bending test. The change in the equivalent bending stiffness of topology-optimized plates compared to the INT-BP is presented in Table 2. The test showed a clear trend that increasing the volume reduction percentage results in reducing the plate's equivalent bending stiffness. The equivalent bending

stiffness decreased around 75% when removing 75% of the INT-BP volume for both screw configurations. The reason for this significant decrease is generally related to the plate's reduced volume. The bone plate's stiffness is one of the major indicators of the implant mechanical behavior during bone healing [44]. Higher plate stiffness means a higher risk of stress being shielded by the plate from the fractured bone, and vice versa. Stress stimuli are one of the key factors to a healthy bone remodeling [45]. Similarly to previous studies, these results confer that the risk of stress shielding phenomenon is minimized [46]. Nevertheless, further investigation is still required which will consider comparing the obtained optimized implants with commercially available implants in terms of their stiffness and biomechanical behavior in a bone-model construct.

Table 2. The equivalent bending stiffness change percentage in comparison to INT-BP plate.

	Equivalent Bending Stiffness Change (%)	
Initial Design	**14.13 ± 1.7 N.m^2**	
Volume Reduction, %	**Plates SC1**	**Plates SC2**
25	−22.29%	−20.99%
50	−32.74%	−27.83%
75	−76.24%	−73.38%

3.3. Biomechanical Stress Analysis

Finite element analysis is an important tool that topology optimization is based on, and it is necessary to simulate highly complicated biomechanical problems. Using the exact same finite element procedure that was initially used to create the topology-optimized plate is a key aspect to validate the results of topology optimization [41,47]. In this paper, a stress analysis study was performed to validate the topology optimization designs by monitoring the stresses at the fracture planes when fixated with the initial and optimized designs. Figure 5 presents the von Mises stress distribution in the region of interest of fracture plane 1 of the eight bone-plate construct FE models for both screw configurations. Table 3 shows the resulting average change in von Mises stresses at the region of interests for all considered bone-plate constructs. In the average stress at the fracture planes, the INT-BP plate under SC1 resulted in 3.98 MPa, while under SC2 it resulted in 13.79 MPa. This is mostly due to the change in the interfragmentary motion of the fracture and the stabilization technique [48]. The reason why this is happening when fixing the distal tibia plate to treat a 43A1.1 fracture with SC1 is due to the bone being stabilized absolutely, while fixing under SC2 results in relative fracture stability, with more interfragmentary motion.

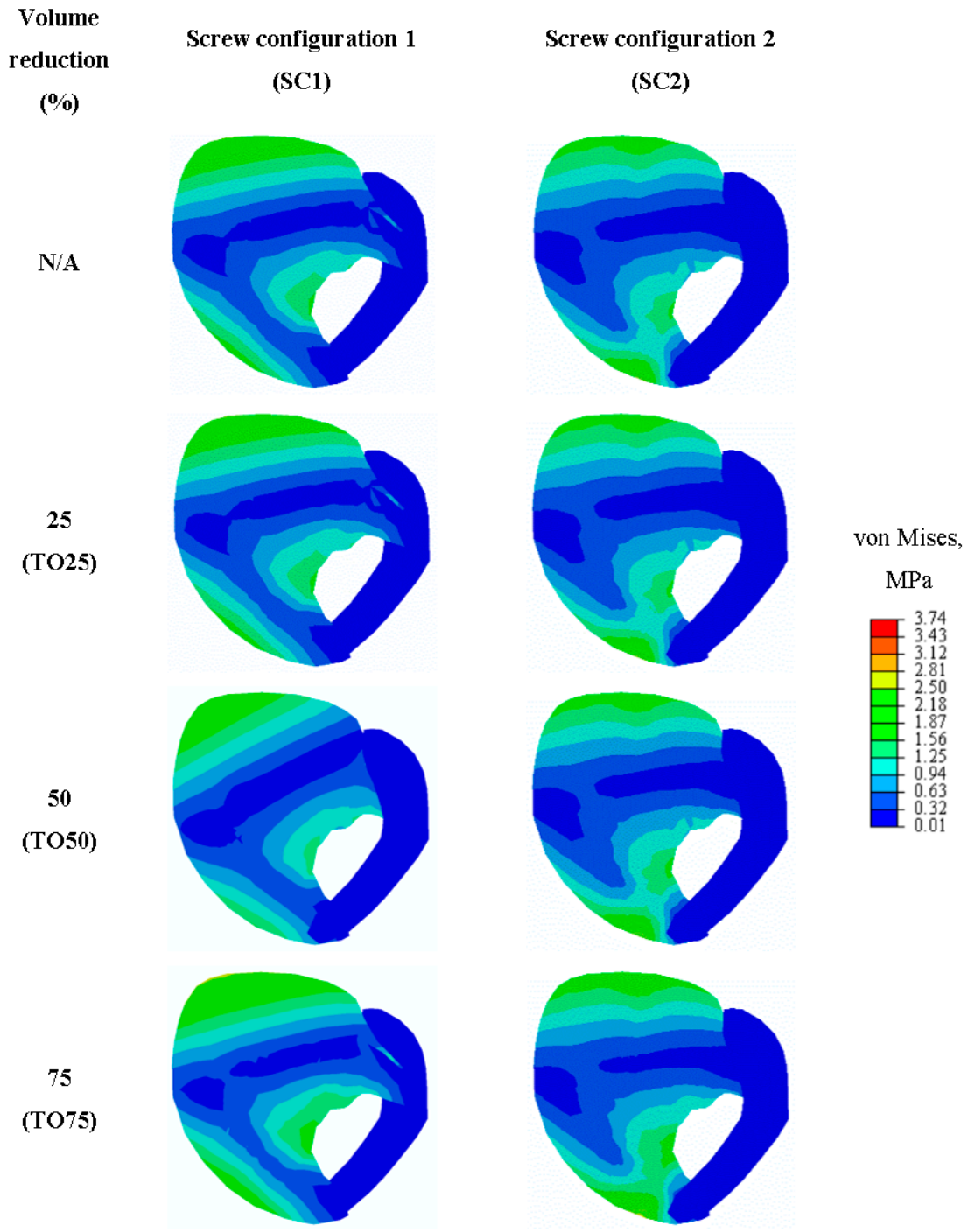

Figure 5. The von Mises stresses at fracture plane 1 for the eight bone-plate models.

Table 3. Average change in the von Mises stresses at the fracture planes of the topology-optimized plates based on the initial designs (INT-BP for SC1 is 3.98 ± 0.23 MPa and INT-BP for SC2 is 13.79 ± 0.19 MPa).

Plate	Von Misses Stress Change (%)	
	SC1	SC2
TO25-BP	0.16	0.09
TO50-BP	2	5
TO75-BP	13	13

3.4. Plate Mechanical Stability

The mechanical stability and stress distribution in Figure 6 shows a clear increasing trend with an increase in the volume reduction of bone plates. The stresses value increased up to 13% with a volume reduction of 75%, considering both screw configurations. This validates the topology optimization (SIMP) algorithm; by maximizing the design's stiffness and controlling its volume reduction, the bone plates are now capable of distributing increased stresses at the fracture region. This is a clear indicator that the stress shielding phenomenon is reducing by optimizing the plates. All plates resulted in less stresses than the tensile strength of the Ti-4Al-6V and presented an acceptable safety factor (SF), which is always intended to be higher than >1 for any design to be accepted [49]. However, further biomechanical parameters such as screw threads must be considered in the finite element model to represent their role on implant-screw load transfer.

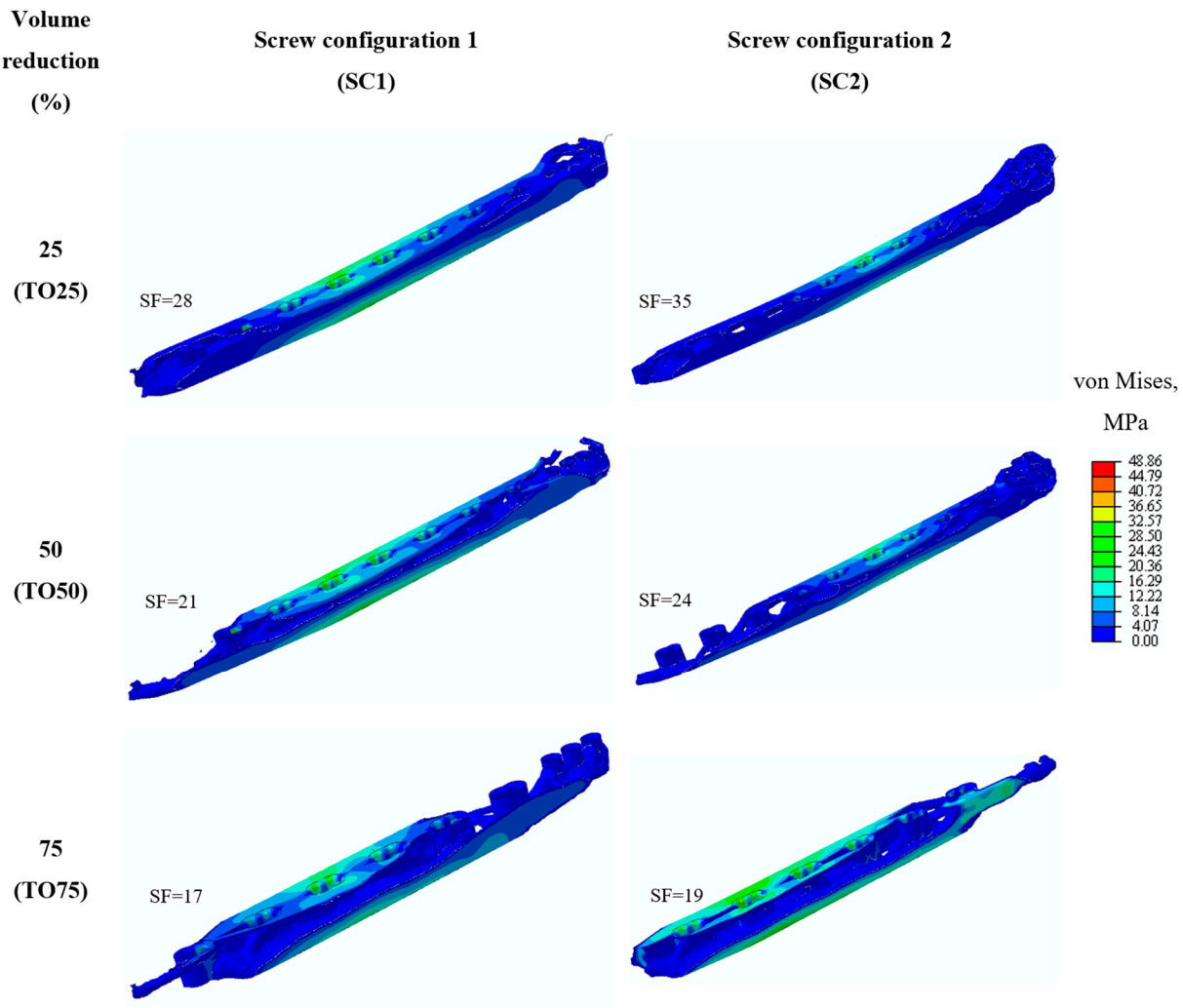

Figure 6. The von Mises stresses on topology optimization plates during spiral fracture fixation.

3.5. Plate Prototyping

Additive manufacturing has become widely popular due to its ability to manufacture complex geometries with topology optimization becoming an important tool in the manufacturing of advanced parts [50]. In a previous study [51], the author presented work verifying and validating the considered finite element analysis by additive manufacturing Ti-4Al-4V topology-optimized generic bone plates in an experimental comparison. This paper used an FFF AM to examine the ability of additive manufacturing to prototype and a produce physical model of an optimized implants. The manufactured implants demon-

strate that additive manufacturing is capable of fabricating the obtained optimal designs of a distal tibia custom-fit plate, as shown in Figure 7. Common FFFs are quite accurate with an XYZ step size of 0.078–0.78 µm, resulting in acceptable geometrical differences between the digital and physical model. FFF is commonly used to produce implants as a plastic prototype to allow the surgeon to visualize the custom-fit implant pre-operation and prepare a surgical plan [52]. However, metal-based additive manufacturing must be explored in future work to validate the designs presented in the study. For example, Iqbal et al. [22] have presented a useful roadmap to optimize and manufacture a pelvic prosthesis using metal additive manufacturing. However, topology optimization technique does not address nor consider additive manufacturing constraints and challenges such as overhanging structures, thermal warping and material anisotropy. Further development on the topology optimization of these implants must consider these constraints prior to fabricating in a metal-based additive manufacturing process.

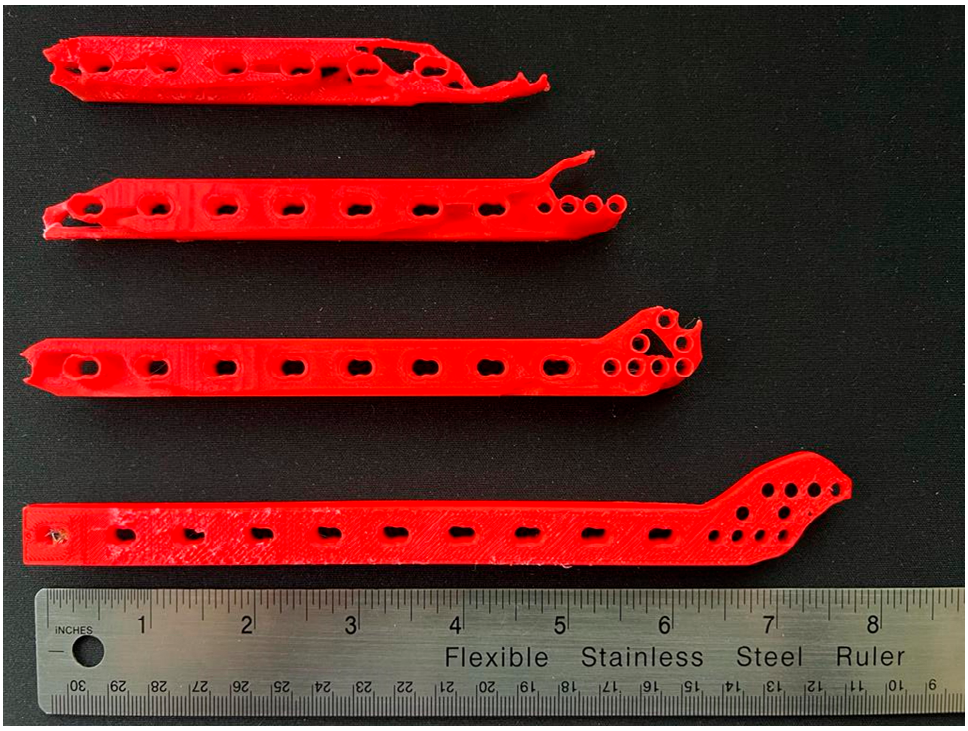

Figure 7. Initial and topology-optimized plates manufactured using fused filament fabrication technique.

4. Conclusions

In this paper, a novel approach combining medical imagining and topology optimization was utilized to redesign a custom-fit distal tibia plate, focusing on reducing post-surgery complications and the risk of stress shielding. The paper concluded with the following:

- Topology optimization is a popular technique to target the stress shielding problem in many different types of implants and has been shown to be a suitable tool. Moreover, topology optimization minimizes the drawbacks of manual iterative design procedures through the use of computer aided design and finite element analysis.
- Topology optimization is capable of redistributing the elemental material of a custom-fit distal tibia plate and results in lightweight plates with less equivalent bending stiffness and, consequently, a more flexible plate design.
- Increasing the effect of topology optimization by increasing the volume reduction led to increased stress stimuli transferred to the bone and reducing the risk of stress shielding, while being able to withstand the biomechanical environment and pre-

senting mechanical stable bone plates for all given topology-optimized plates in both screw configurations.
- Topology optimization presented the ability to design for different screw configurations and enabling the alteration of the behavior of the bone fixation, with SC1 optimal designs providing absolute stability and minimal interfragmentary motion, whilst the SC2 optimal designs providing relative stability with interfragmentary motion. This shows that topology optimization is a suitable tool for pre-surgical planning.
- Rapid prototyping presented the ability to create visual prototypes of the intricate designs obtained from topology optimization and to assist with the planning of the surgical operation.

Funding: This research received no external funding.

Institutional Review Board Statement: Not applicable.

Informed Consent Statement: Not applicable.

Acknowledgments: The author acknowledges the Researchers Supporting Project number (RSP-2021/299), King Saud University, Riyadh, Saudi Arabia. The author is grateful for the support provided by Mohammed Al-Qahtani, University of Manchester, Manchester, UK and Chris Peach, Manchester University Foundation NHS Trust, Manchester, UK for the patient's data, and Abdullah Al-Theyab, Prince Mohammed Bin Abdulaziz Hosptial (PMAH), Riyadh, Saudi Arabia for the clinical advice.

Conflicts of Interest: The authors declare no conflict of interest.

References

1. Miller, D.L.; Goswami, T. A review of locking compression plate biomechanics and their advantages as internal fixators in fracture healing. *Clin. Biomech.* **2007**, *22*, 1049–1062. [CrossRef]
2. Sommer, C.; Gautier, E.; Müller, M.; Helfet, D.L.; Wagner, M. First clinical results of the Locking Compression Plate (LCP). *Injury* **2003**, *34* (Suppl. 2), B43–B54. [CrossRef] [PubMed]
3. Prasad, K.; Bazaka, O.; Chua, M.; Rochford, M.; Fedrick, L.; Spoor, J.; Symes, R.; Tieppo, M.; Collins, C.; Cao, A.; et al. Metallic Biomaterials: Current Challenges and Opportunities. *Materials* **2017**, *10*, 884. [CrossRef] [PubMed]
4. Ridzwan, M.I.Z.; Shuib, S.; Hassan, A.Y.; Shokri, A.A.; Ibrahim, M.N.M. Problem of stress shielding and improvement to the hip implant designs: A review. *J. Med. Sci.* **2007**, *7*, 460–467. [CrossRef]
5. Elias, C.N.; Lima, J.H.C.; Valiev, R.; Meyers, M.A. Biomedical applications of titanium and its alloys. *JOM* **2008**, *60*, 46–49. [CrossRef]
6. Hanson, B.; van der Werken, C.; Stengel, D. Surgeons' beliefs and perceptions about removal of orthopaedic implants. *BMC Musculoskel. Disord.* **2008**, *9*, 73. [CrossRef] [PubMed]
7. Hofmann, G.O. Biodegradable implants in orthopaedic surgery—A review on the state-of-the-art. *Clin. Mater.* **1992**, *10*, 75–80. [CrossRef]
8. Inion. *Economic Benefit of Biodegradable Ankle Fracture Fixation*; Inion OY: Tampere, Finland, 2015.
9. Manavitehrani, I.; Fathi, A.; Badr, H.; Daly, S.; Negahi Shirazi, A.; Dehghani, F. Biomedical Applications of Biodegradable Polyesters. *Polymers* **2016**, *8*, 20. [CrossRef]
10. Prakasam, M.; Locs, J.; Salma-Ancane, K.; Loca, D.; Largeteau, A.; Berzina-Cimdina, L. Biodegradable Materials and Metallic Implants—A Review. *J. Funct. Biomater.* **2017**, *8*, 44. [CrossRef] [PubMed]
11. Weisgrab, G.; Guillaume, O.; Guo, Z.; Heimel, P.; Slezak, P.; Poot, A.; Grijpma, D.; Ovsianikov, A. 3D Printing of large-scale and highly porous biodegradable tissue engineering scaffolds from poly(trimethylene-carbonate) using two-photon-polymerization. *Biofabrication* **2020**, *12*, 045036. [CrossRef]
12. Hou, Y.; Wang, W.; Bartolo, P. Investigation of polycaprolactone for bone tissue engineering scaffolds: In vitro degradation and biological studies. *Mater. Des.* **2022**, *216*, 110582. [CrossRef]
13. Rama Krishna, K.; Sridhar, I.; Sivashanker, S.; Khong, K.S.; Ghista, D.N. Design of Fracture Fixation Plate for Necessary and Sufficient Bone Stress Shielding. *JSME Int. J.* **2004**, *47*, 1086–1094. [CrossRef]
14. Galbusera, F.; Bertolazzi, L.; Balossino, R.; Dubini, G. Combined computational study of mechanical behaviour and drug delivery from a porous, hydroxyapatite-based bone graft. *Biomech. Model. Mechanobiol.* **2009**, *8*, 209–216. [CrossRef] [PubMed]
15. Rendenbach, C.; Sellenschloh, K.; Gerbig, L.; Morlock, M.M.; Beck-Broichsitter, B.; Smeets, R.; Heiland, M.; Huber, G.; Hanken, H. CAD-CAM plates versus conventional fixation plates for primary mandibular reconstruction: A biomechanical in vitro analysis. *J. Cranio-Maxillofac. Surg.* **2017**, *45*, 1878–1883. [CrossRef] [PubMed]
16. Gutwald, R.; Jaeger, R.; Lambers, F.M. Customized mandibular reconstruction plates improve mechanical performance in a mandibular reconstruction model. *Comput. Methods Biomech. Biomed. Eng.* **2017**, *20*, 426–435. [CrossRef] [PubMed]

17. Attard, A.; Tawy, G.F.; Simons, M.; Riches, P.; Rowe, P.; Biant, L.C. Health costs and efficiencies of patient-specific and single-use instrumentation in total knee arthroplasty: A randomised controlled trial. *BMJ Open Qual.* **2019**, *8*, e000493. [CrossRef] [PubMed]
18. Yam, M.G.J.; Chao, J.Y.Y.; Leong, C.; Tan, C.H. 3D printed patient specific customised surgical jig for reverse shoulder arthroplasty, a cost effective and accurate solution. *J. Clin. Orthop. Trauma* **2021**, *21*, 101503. [CrossRef] [PubMed]
19. Ridzwan, S.; Hassan, A.Y.; Shokri, A.A.; Ibrahim, M.N.M. Optimization in Implant Topology to Reduce Stress Shielding Problem. *J. Appl. Sci.* **2006**, *6*, 2768–2773.
20. Park, S.-M.; Park, S.; Park, J.; Choi, M.; Kim, L.; Noh, G. Design process of patient-specific osteosynthesis plates using topology optimization. *J. Comput. Des. Eng.* **2021**, *8*, 1257–1266. [CrossRef]
21. Zhang, A.; Chen, H.; Liu, Y.; Wu, N.; Chen, B.; Zhao, X.; Han, Q.; Wang, J. Customized reconstructive prosthesis design based on topological optimization to treat severe proximal tibia defect. *Bio-Des. Manuf.* **2021**, *4*, 87–99. [CrossRef]
22. Iqbal, T.; Wang, L.; Li, D.; Dong, E.; Fan, H.; Fu, J.; Hu, C. A general multi-objective topology optimization methodology developed for customized design of pelvic prostheses. *Med. Eng. Phys.* **2019**, *69*, 8–16. [CrossRef]
23. Fraldi, M.; Esposito, L.; Perrella, G.; Cutolo, A.; Cowin, S.C. Topological optimization in hip prosthesis design. *Biomech. Model. Mechanobiol.* **2010**, *9*, 389–402. [CrossRef] [PubMed]
24. Al-Tamimi, A.A. 3D Topology Optimization and Mesh Dependency for Redesigning Locking Compression Plates Aiming to Reduce Stress Shielding. *Int. J. Bioprinting* **2021**, *7*, 339. [CrossRef]
25. Chuah, H.G.; Rahim, I.A.; Yusof, M.I. Topology optimisation of spinal interbody cage for reducing stress shielding effect. *Comput. Methods Biomech. Biomed. Eng.* **2010**, *13*, 319–326. [CrossRef] [PubMed]
26. Liu, Y.-F.; Fan, Y.-Y.; Jiang, X.-F.; Baur, D.A. A customized fixation plate with novel structure designed by topological optimization for mandibular angle fracture based on finite element analysis. *BioMedical Eng. OnLine* **2017**, *16*, 131. [CrossRef] [PubMed]
27. Al-Tamimi, A.A.; Hernandez, M.A.; Omar, A.; Morales-Aldana, D.F.; Peach, C.; Bartolo, P. Mechanical, biological and tribological behaviour of fixation plates 3D printed by electron beam and selective laser melting. *Int. J. Adv. Manuf. Technol.* **2020**, *109*, 673–688. [CrossRef]
28. Siva Rama Krishna, L.; Mahesh, N.; Sateesh, N. Topology optimization using solid isotropic material with penalization technique for additive manufacturing. *Mater. Today Proc.* **2017**, *4*, 1414–1422. [CrossRef]
29. Klahn, C.; Leutenecker, B.; Meboldt, M. Design Strategies for the Process of Additive Manufacturing. *Procedia CIRP* **2015**, *36*, 230–235. [CrossRef]
30. Parthasarathy, J. Additive manufacturing of medical devices. In *Additive Manufacturing Innovations, Advances, and Applications*; Sudarshan, T.S., Ed.; CRC Press: Boca Raton, FL, USA, 2015; pp. 369–388.
31. Murr, L.E. Frontiers of 3D Printing/Additive Manufacturing: From Human Organs to Aircraft Fabrication†. *J. Mater. Sci. Technol.* **2016**, *32*, 987–995. [CrossRef]
32. Tilton, M.; Lewis, G.S.; Bok Wee, H.; Armstrong, A.; Hast, M.W.; Manogharan, G. Additive manufacturing of fracture fixation implants: Design, material characterization, biomechanical modeling and experimentation. *Additiv. Manuf.* **2020**, *33*, 101137. [CrossRef]
33. Meinberg, E.G.; Agel, J.; Roberts, C.S.; Karam, M.D.; Kellam, J.F. Fracture and Dislocation Classification Compendium-2018. *J. Orthop. Trauma* **2018**, *32* (Suppl. 1), S1–S170. [CrossRef] [PubMed]
34. LCP Distal Tibia Plate. Available online: https://www.jnjmedtech.com/en-US/product/35mm-lcp-medial-distal-tibia-plate (accessed on 23 August 2022).
35. Bendsøe, M.P.; Sigmund, O. Topology optimization by distribution of isotropic material. In *Topology Optimization: Theory, Methods, and Applications*; Springer: Berlin/Heidelberg, Germany, 2004; pp. 1–69.
36. Ferro, N.; Perotto, S.; Bianchi, D.; Ferrante, R.; Mannisi, M. Design of cellular materials for multiscale topology optimization: Application to patient-specific orthopedic devices. *Struct. Multidiscip. Optim.* **2022**, *65*, 79. [CrossRef]
37. Al-Tamimi, A.; Fernandes, P.R.A.; Peach, C.; Cooper, G.; Diver, C.; Bartolo, P.J. Metallic bone fixation implants: A novel design approach for reducing the stress shielding phenomenon. *Virtual Phys. Prototyp.* **2017**, *12*, 141–151. [CrossRef]
38. Kim, S.-H.; Chang, S.-H.; Son, D.-S. Finite element analysis of the effect of bending stiffness and contact condition of composite bone plates with simple rectangular cross-section on the bio-mechanical behaviour of fractured long bones. *Compos. Part B Eng.* **2011**, *42*, 1731–1738. [CrossRef]
39. Wang, S.-P.; Lin, K.-J.; Hsu, C.-E.; Chen, C.-P.; Shih, C.-M.; Lin, K.-P. Biomechanical Comparison of a Novel Implant and Commercial Fixation Devices for AO/OTA 43-C1 Type Distal Tibial Fracture. *Appl. Sci.* **2021**, *11*, 4395. [CrossRef]
40. AO Foundation. Available online: https://www.aofoundation.org/trauma/clinical-library-and-tools/journals-and-publications/classification (accessed on 23 August 2022).
41. Al-Tamimi, A.A.; Quental, C.; Folgado, J.; Peach, C.; Bartolo, P. Stress analysis in a bone fracture fixed with topology-optimised plates. *Biomech. Model. Mechanobiol.* **2020**, *19*, 693–699. [CrossRef]
42. *BS 3531-23.1:1991*; Implants for Osteosynthesis. Bone Plates Method for Determination of Bending Strength and Stiffness. British Standards Institution: London, UK, 1991.
43. Minns, R.J.; Bremble, G.R.; Campbell, J. A biomechanical study of internal fixation of the tibial shaft. *J. Biomech.* **1977**, *10*, 569–579. [CrossRef]
44. Ganesh, V.K.; Ramakrishna, K.; Ghista, D.N. Biomechanics of bone-fracture fixation by stiffness-graded plates in comparison with stainless-steel plates. *BioMedical Eng. OnLine* **2005**, *4*, 46. [CrossRef]

45. Wippert, P.-M.; Rector, M.; Kuhn, G.; Wuertz-Kozak, K. Stress and Alterations in Bones: An Interdisciplinary Perspective. *Front. Endocrinol.* **2017**, *8*, 96. [CrossRef] [PubMed]
46. Wu, N.; Li, S.; Zhang, B.; Wang, C.; Chen, B.; Han, Q.; Wang, J. The advances of topology optimization techniques in orthopedic implants: A review. *Med. Bio.l Eng. Comput.* **2021**, *59*, 1673–1689. [CrossRef]
47. Lang, J.J.; Bastian, M.; Foehr, P.; Seebach, M.; Weitz, J.; von Deimling, C.; Schwaiger, B.J.; Micheler, C.M.; Wilhelm, N.J.; Grosse, C.U.; et al. Improving mandibular reconstruction by using topology optimization, patient specific design and additive manufacturing?-A biomechanical comparison against miniplates on human specimen. *PLoS ONE* **2021**, *16*, e0253002. [CrossRef] [PubMed]
48. Ruedi, T.; Buckley, R.E.; Moran, C.G. *AO Principles of Fracture Management-Vol. 1: Principles-Vol. 2: Specific Fractures*, 3rd ed.; Thieme: Stuttgart, Germany, 2018.
49. Liao, B.; Sun, J.; Xu, C.; Xia, R.; Li, W.; Lu, D.; Jin, Z. A mechanical study of personalised Ti6Al4V tibial fracture fixation plates with grooved surface by finite element analysis. *Biosurface Biotribology* **2021**, *7*, 142–153. [CrossRef]
50. Gibson, I.; Rosen, D.; Stucker, B.; Khorasani, M. *Additive Manufacturing Technologies*, 3rd ed.; Springer Nature: Cham, Switzerland, 2021; p. 675.
51. Al-Tamimi, A.; Huang, B.; Vyas, C.; Hernandez, M.; Peach, C.; Bartolo, P. Topology optimised metallic bone plates produced by electron beam melting: A mechanical and biological study. *Int. J. Adv. Manuf. Technol.* **2019**, *104*, 195–210. [CrossRef]
52. Segaran, N.; Saini, G.; Mayer, J.L.; Naidu, S.; Patel, I.; Alzubaidi, S.; Oklu, R. Application of 3D Printing in Preoperative Planning. *J. Clin. Med.* **2021**, *10*, 917. [CrossRef]